ELSEVIER

April 1998

Materials Letters 35 (1998) 39–49

MATERIALS LETTERS

Thin-layer composite unimorph ferroelectric driver and sensor properties

Karla M. Mossi [a,*], Gregory V. Selby [b], Robert G. Bryant [c]

[a] *Face International Corporation, 427 W 35th St., Norfolk, VA 23508, USA*
[b] *Mechanical Engineering Department, Old Dominion University, Norfolk, VA 23529, USA*
[c] *NASA Langley Research Center, Mail Stop 226, Hampton, VA 23681-0001, USA*

Received 8 August 1997; accepted 15 August 1997

Abstract

Tests were conducted on 13 different configurations of a new class of piezoelectric devices called THUNDER (thin-layer composite unimorph ferroelectric driver and sensor). These configurations consisted of a combination of 1, 3, 5, 7, and 9 layers of 25.4 μm thick aluminum as backing material, with and without a top layer of 25.4 μm aluminum. All of these configurations used the same piezoelectric ceramic wafer (PZT-5A) with dimensions of $5.08 \times 3.81 \times 0.018$ cm. The above configurations were tested at two stages of the manufacturing process: before and after re-poling. The parameters measured included frequency, driving voltage, displacement, capacitance, and radius of curvature. An optic sensor recorded the displacement at a fixed voltage (100–400 V peak-to-peak), over a predetermined frequency range (1–1000 Hz). These displacement measurements were performed using a computer that controlled the process of activating and measuring the displacement of the device. A parameter α was defined which can be used to predict which configuration will produce the most displacement for a free standing device. © 1998 Elsevier Science B.V.

PACS: 77.55.+f; 77.65.Bn; 77.84.Dy
Keywords: Piezoelectric device; Ferroelectric; Optic; Displacement; Optical sensor; Poled ceramic wafers; PZT; Actuator; THUNDER

1. Introduction

During the past few years, a significant amount of research has been performed on the control of flexible structures through smart sensors and actuators [1–3]. Some of these systems can sense changes in their environment and respond accordingly [4,5]. Such developments promote the evolution of smart systems which have demonstrated effectiveness either as passive or active control systems in many applications. Depending on the desired application, these devices can replace some functions presently performed by mechanical actuators, and have the advantage over mechanical systems in weight and volume. [5,7] Smart structures are made with adaptive materials that can change their properties (i.e., stiffness, shape, etc.) in response to the application of an external stimulus (such as electricity, heat or a magnetic field) [6]. When an electric field is applied to certain phases of a piezoelectric crystal, the crystal undergoes a physical distortion [7]. In order for a piezoelectric interaction to exist, it is necessary that certain axes possess polarity [10]. Such polarity can

* Correspondence author. Fax: +1-757-6242128.

PII S0167-577X(97)00214-0

be permanently induced in isotropic polycrystalline ceramics by applying a strong DC electric field. The process of applying an electric field is referred to as *poling*.

Lead titanate zirconate ($Pb(Zr, Ti)O_3$) or PZT and its modified forms, are the most used piezoceramics in various solid solutions. This is because of their high degree of orientation and spontaneous polarization, combined with high permanent polarization and high dielectric constant [8,9]. A variety of PZT materials have been developed to suit a wide range of signal transmission and reception qualities, and applications of piezoelectric materials used as actuators have been studied in recent years [10,11]. Among PZT actuators are unimorphs™, bimorphs™, reduced and internally biased oxide wafer (RAINBOW™), and a new device called thin-layer composite unimorph ferroelectric driver and sensor (THUNDER) [12,16]. Unimorphs™ are simple large displacement actuators that are created by bonding a PZT strip to a thin metal strip. Bimorphs™ consist of two electrically opposed PZT strips bonded together that change directions with applied voltage. A RAINBOW ceramic is a monolithic structure with an integral electrode that is fabricated to place an internal compressive stress bias on the piezoelectric element [13,14]. The new piezoelectric device, THUNDER, developed at NASA Langley Research Center, is composed of a ferroelectric material which is prestressed against a foundation material (glass, metal, etc). This new piezoelectric device is based on a piezoelectric ceramic wafer attached to a metal backing using a polyimide adhesive [16]. The ferroelectric material used in the manufacture consists of a piezoelectric wafer laminated between layers of materials, such as aluminum, stainless steel, beryllium, etc., bonded with a soluble imide adhesive created at NASA [15,16]. In this manner, a more durable, rugged, and more flexible actuator is obtained [17–21]. Two clear advantages of this new piezoelectric device class over others are ease of fabrication and the ability to create application specific devices.

2. Experimental setup

The electromechanical characterization of the present class of piezoelectric devices was performed at NASA Langley Research Center using a data acquisition system composed of computer controlled hardware and software that provided flexibility in measuring the pertinent parameters. The hardware used included a portable computer equipped with an IEEE 488 interface card; a Wavetek Synthesized Function Generator (Model 23) with an IEEE interface; a TREK Power Supply/ Amplifier (Model 70/750); an optical-fiber-based Angstrom Resolver Series (Dual Channel Model 201); a Dual Channel Low Pass Filter (Model SR640); a Hewlett-Packard 4-channel Oscilloscope (HP54601A with an IEEE interface); and a Hewlett Packard Impedance Analyzer (HP-4192A with an IEEE interface). All of the hardware was monitored and controlled using LabVIEW™ software.

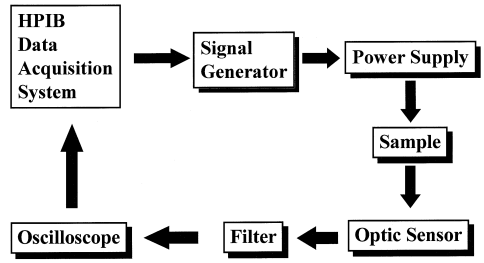

Fig. 1. Experimental setup control loop.

A schematic of the control loop for displacement measurements is presented in Fig. 1. This control loop is composed of the computer, which is connected to the function generator that controls the power supply to drive the piezoelectric device. The optic sensor measures the displacement through a filtered signal fed back to the computer through a digitizing oscilloscope.

3. Manufacturing process

3.1. Materials

The raw materials needed to manufacture the present THUNDER devices are a piezoelectric ceramic wafer, metallic backing material, and an adhesive in spray and film form. The wafers used in this study were all Morgan Matroc PZT-5A ($6.35 \times 3.81 \times 0.018$ cm) and several different thicknesses of aluminum as backing material (from commercial

vendors) were used. The construction of the piezoelectric devices required additional equipment which included an air brush, an oven with a vacuum fixture and an operating temperature of 350°C, and an autoclave with a minimum capability of 207 kPa (30 psi) and 350°C.

3.2. Procedure for the fabrication of THUNDER

There are five basic steps involved in manufacturing the present class of piezoelectric devices: (1) spray coating of the ceramics, (2) construction of layers, (3) assembly, (4) pre-bonding, and, (5) final bonding process in an autoclave.

3.3. Spray coating of the ceramics

LaRC-SI™/*N*-methyl-pyrolidinone 10 wt% solution (Imitec), is sprayed using an air brush. Both sides of the ceramic are cleaned using alcohol. Two coats are then sprayed on each side of the ceramic which is then dried in an oven for 2 h at 70°C.

3.4. Construction of the layers

The backing material is first cleaned using alcohol, roughened with sandpaper, and sprayed with the LaRC-SI™ solution. The materials (backing and LaRC-SI film, 3% offset) are cut to the desired size. The spraying of the backing materials is the same as above.

3.5. Assembly

The materials are assembled in the required order and thermally processed to produce the piezoelectric devices. The order of the layers, starting from the bottom for a particular device is metal, LaRC-SI film, metal, LaRC-SI film, ceramic wafer, LaRC-SI film, and top metallic layer (optional). See Fig. 2 for an schematic of the new piezoelectric device assembly.

3.6. Pre-bonding

An aluminum plate with a layer of fiberglass cloth and Kapton™ polyimide film coated with Frekote™ release agent. These layers are concentrically put on

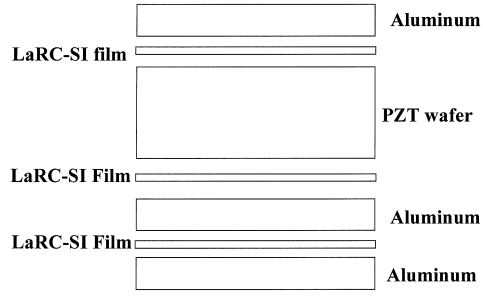

Fig. 2. Schematic of the new piezoelectric device assembly.

the plate, leaving a border of approximately 2.54 cm. The assembly is carefully placed on the plate, with additional layers on top of it of and coated Kapton™ film and fiberglass cloth. Around the outer edge of the plate, heat resistant sealant tape is placed and a vacuum port is attached inside the tape perimeter. Kapton™ film is placed over the tape covering the entire surface of the plate and pressed around the tape to ensure a good seal. The entire plate is then put into an oven for 1 h at 325°C. When the temperature is lowered to 180°C, the vacuum is released and the assembly is allowed to cool down to ambient temperature.

3.7. Autoclave

A plate again is prepared in the same manner that for the oven process, and put into an autoclave. The temperature is raised to 320°C at 5°C/min intervals with a full vacuum. At 320°C, a pressure of 207 kPa (30 psi) is placed for 30 min and then the plate is cooled down at a rate of 5°C/min cooling rate until the temperature reaches 200°C. The vacuum is then released and the fixture is allowed to cool to ambient temperature where upon the devices are removed.

4. Results

The THUNDER devices were clamped using modeling clay in its four corners. The driving voltage was varied between 100 and 400 Vpp (peak-to-peak voltage) in 50 V increments and the frequency was varied between 1 and 1000 Hz for each case tested. The wafer configurations included aluminum of different thicknesses and number of layers. Each

Table 1
Test configurations

Config.	Designation	Top layer	Bottom layers
1	0/1–x/Al[a]	none	1 layer of Al
2	0/3–x/Al[a]	none	3 layers of Al
3	0/5–x/Al[a]	none	5 layers of Al
4	0/7–x/Al[a]	none	7 layers of Al
5	0/9–x/Al[a]	none	9 layers of Al
6	1/3–Al/Al[a]	1 layer of Al	3 layers of Al
7	1/5–Al/Al[a]	1 layer of Al	5 layers of Al
8	1/7–Al/Al[a]	1 layer of Al	7 layers of Al
9	1/9–Al/Al[a]	1 layer of Al	9 layers of Al

[a]1 mil (25.4 μm = 0.0254 mm) layers of Al.

configuration had a 1-mil layer of LaRC-SI film between the layers and all materials were sprayed with LaRC-SI solution. All the metallic materials used were 25.4 μm thick, except where noted. A summary of the configurations tested is presented in Table 1.

In order to verify that piezoelectric device displacement performance was independent of the degree of poling of the devices, tests were performed before and after the devices were re-poled. Poling was performed with a dc voltage of 420 V, applied for 5 min to each device. The poling time of 5 min was chosen because the capacitance of the piezoelectric device was found to be constant for poling times of 1, 3, 5, and 10 min.

Before poling, displacement performance of the various configurations before re-poling, data were examined at three values of frequency (1, 10, and 100 Hz) at 200 Vpp and arranged per categories. Taking into account all configurations that do not have a layer of material on top of the ceramic wafer (designated as x/Al) and using the theoretical backing thickness of the piezoelectric device, Fig. 3 was produced. This figure generally indicates an increase in device displacement as the number of layers of backing material is increased, except for the configuration with 5 layers of backing material. This may be due to a defective ceramic piece. This graph also shows that when the backing material exceeds 7 layers, the displacement decays. The theoretical bottom thickness was determined in the following manner:

Configuration 3 (0/3–x/Al) means 3 layers of backing material with a bottom thickness of 3-mil.

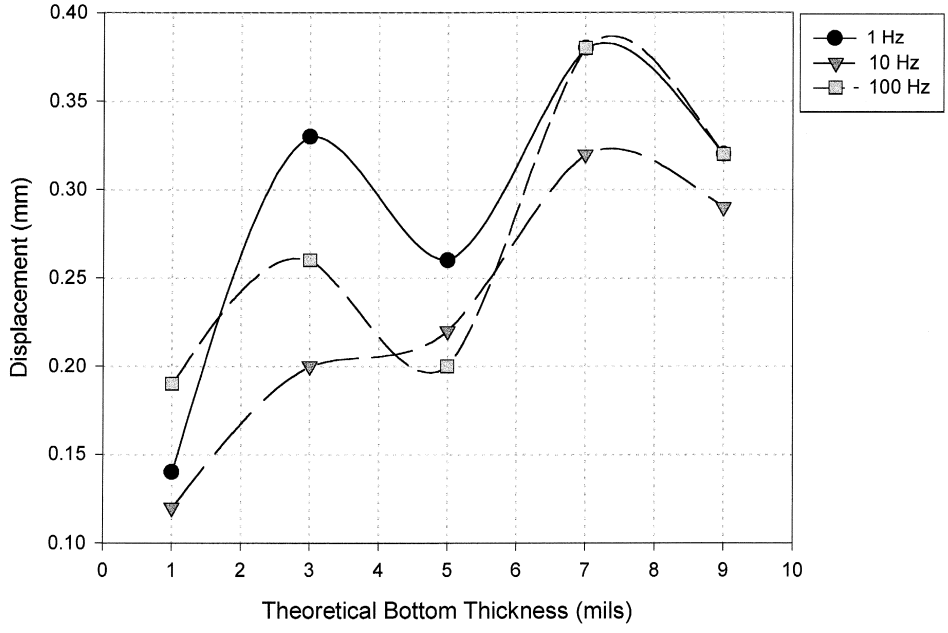

Fig. 3. Displacement of x/Al configurations vs. theoretical total bottom-layer thickness at 1, 10, and 100 Hz, and 200 Vpp, before re-poling.

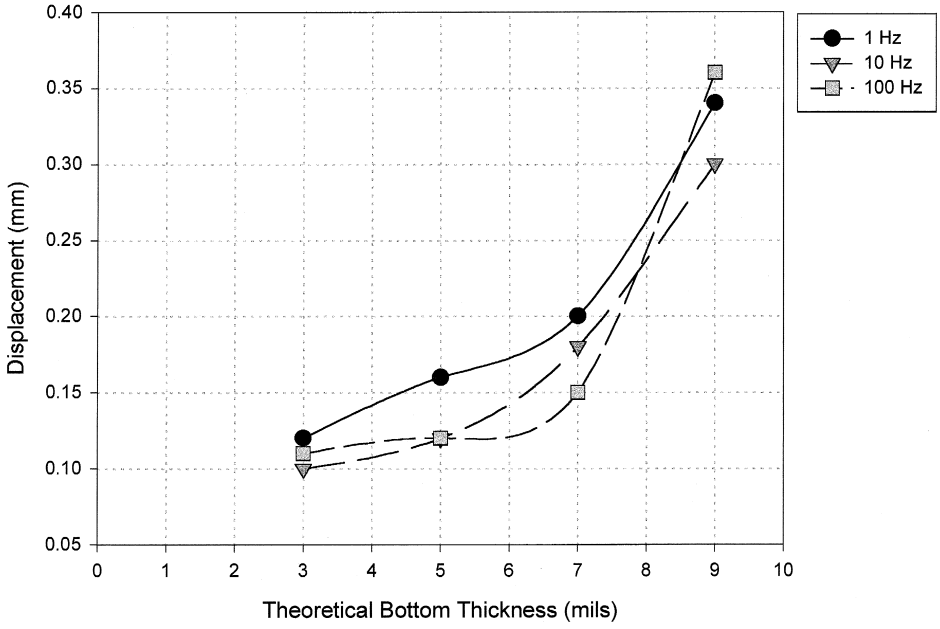

Fig. 4. Displacement of Al/Al configurations vs. theoretical total bottom-layer thickness at 1, 10, and 100 Hz, and 200 Vpp, before re-poling.

The same data for configurations with a metallic top layer (Al/Al configurations) are presented in Fig. 4. It is evident that displacement for Al/Al configurations is generally significantly less than for x/Al configurations, indicating that the top layer of material restricts the movement of the piezoelectric device.

After re-poling, capacitance as well as displacement measurements were performed on all configurations. Capacitance and displacement were measured as a function of frequency (between 1 and 1000 Hz) at fixed voltages. A graph displaying a sample of the changes in capacitance at the different manufacturing stages is presented in Fig. 5. Dis-

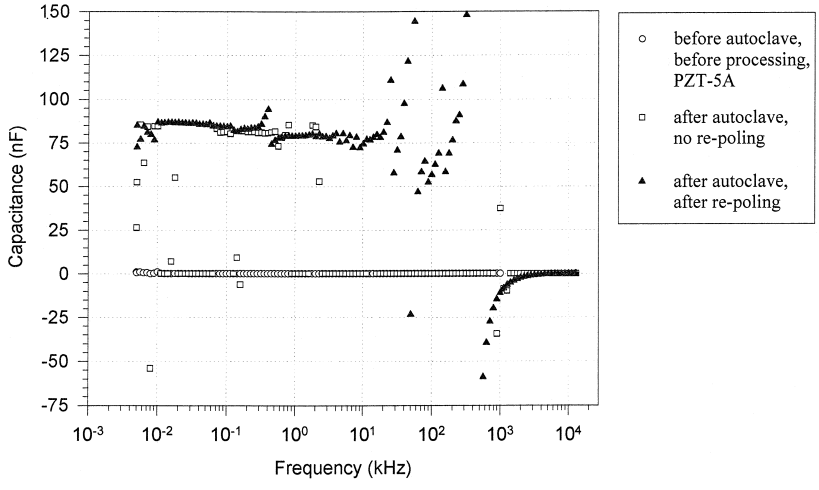

Fig. 5. Capacitance vs. frequency for configurations 0/5–x/Al at different processing stages.

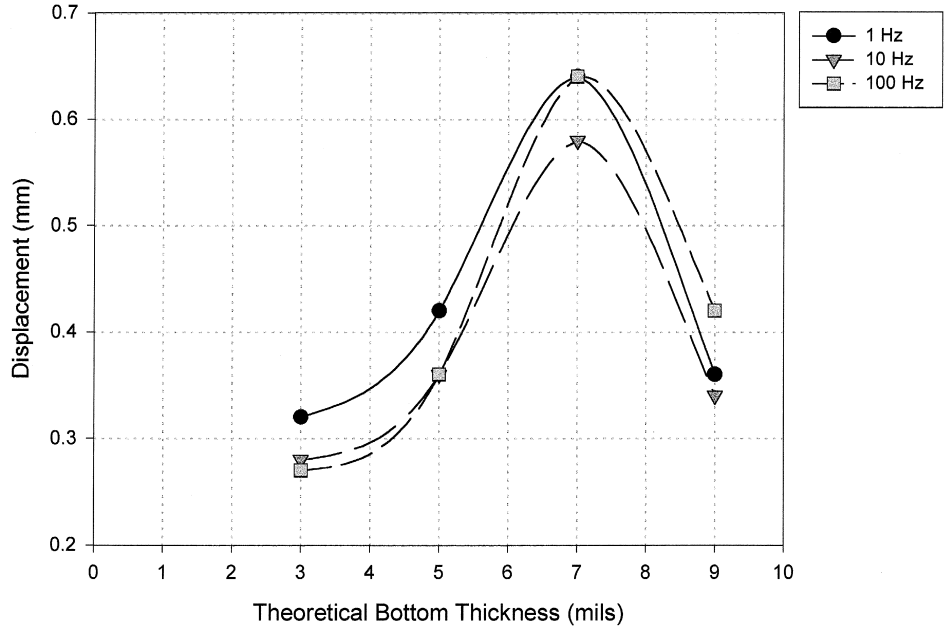

Fig. 6. Displacement of x/Al configurations vs. theoretical total bottom-layer thickness at 1, 10, and 100 Hz, and 200 Vpp, after re-poling.

placement measurements show a clear relationship between the total bottom layer thickness and device displacement performance, Figs. 6 and 7, as well as an overall performance improvement over the results obtained before re-poling. In addition, a different trend is shown for the Al/Al configurations in Fig.

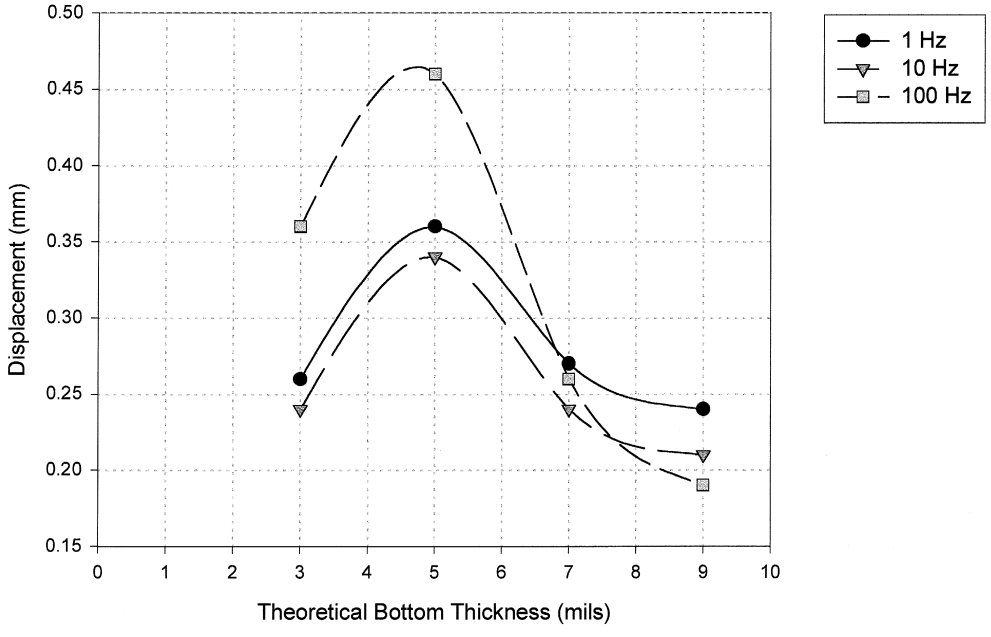

Fig. 7. Displacement of Al/Al configurations vs. theoretical total bottom-layer thickness at 1, 10, and 100 Hz, and 200 Vpp, after re-poling.

7, as compared to the results for the same configuration as shown in Fig. 4. The latter pattern is in better agreement with data for the x/Al configurations.

From all the tests performed, it was observed that the resonant frequency for most configurations tested occurred between 100 and 200 Hz, suggesting that the resonant frequency is independent of configuration (thickness, driving voltage, etc.), and degree of poling. This phenomenon implies that resonant frequency is independent of the variables examined in the present research. Therefore, it is most likely a result of device geometry and fixturing.

In order to explain the relationship between the number of backing layers and displacement performance, a theory based on the neutral axis of a curved beam is suggested. Furman, Li, and Haertling [22] have presented a similar theory for a different class of pre-stressed piezoelectric actuators (RAINBOW™). This actuator is composed of an active layer (oxide layer) and an inactive one (reduced layer). They predicted that the maximum displacement should occur for an active/inactive layer thickness ratio of approximately one. This theory is based on neutral axis location.

The location of the neutral axis is found by using [23]

$$R = \frac{A}{\int_A \mathrm{d}A/r} \tag{1}$$

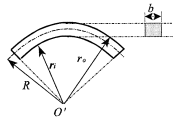

where R is the location of the neutral axis, from the center of curvature (O′) of the member, A is the cross-sectional area, r is the arbitrary position of the element $\mathrm{d}A$ from the center (O′). Since all the specimens tested had the same cross-sectional area, Eq. (1) above becomes Eq. (2),

$$R = \frac{(r_o - r_i)}{\ln[r_o/r_i]} \tag{2}$$

where R is the location of the neutral axis, r_i = inner specimen radius, and r_o = outer specimen radius (calculated from geometry).

Table 2
Location of neutral axis for x/Al configurations using theoretical thickness

Conf.	r_i	Theoretical thickness (mils)				R	$R - r_i$	α	β
	(in)	top	ceramic	bottom	total	(in)	(mils)		
1	6.0	0	7	1	8	6.004	4.0	7.00	4.0
2	6.5	0	7	3	10	6.500	5.0	2.33	1.7
3	5.4	0	7	5	12	5.400	6.0	1.40	1.2
4	6.2	0	7	7	14	6.200	7.0	1.00	1.0
5	6.3	0	7	9	16	6.300	8.0	0.78	0.9

In order to compare all the cases, two ratios are defined. First, the 'active to inactive' ratio is defined as used for the RAINBOW™ devices. For simplicity, this ratio (Eq. (3)) is defined as:

$$\beta = \text{active layer thickness} / \text{inactive layer thickness} \tag{3}$$

or

$$\beta = (\text{top layers} + \text{ceramic thickness}) / \text{backing layers total thickness}$$

Then, a second ratio (Eq. (4)) is defined, which refers to the location of the neutral axis of the element:

$$\alpha = (R - r_i) / \text{inactive layer thickness} \tag{4}$$

where r_i is the radius of curvature of the sample.

Using the above relations, the neutral axis of each specimen can be calculated. Only configurations after re-poling were considered, since there is more

Table 3
Location of neutral axis for x/Al configurations using measured thickness

Conf.	r_i	Estimated thickness of the 'active' layer (mils)	Measured total thickness (mils)	R (in)	$R - r_i$ (mils)	α	β
1	6.0	7	11.0	6.005	5.5	1.37	1.8
2	6.5	7	16.0	6.508	8.0	0.89	0.8
3	5.4	7	17.5	5.409	8.7	0.83	0.7
4	6.2	7	18.5	6.209	9.2	0.80	0.6
5	6.3	7	22.0	6.311	11.0	0.73	0.5

Table 4
Location of neutral axis for Al/Al configurations using theoretical thickness

Conf.	r_i	Theoretical thickness (mils)				R	$R - r_i$	α	β
	(in)	top	ceramic	bottom	total	(in)	(mils)		
6	6.0	1	7	3	11	6.029	5.5	2.67	1.80
7	4.7	1	7	5	13	4.731	6.5	1.60	1.30
8	7.3	1	7	7	15	7.291	7.5	1.14	1.07
9	5.9	1	7	9	17	5.914	8.5	0.88	0.94

Table 5
Location of neutral axis for Al/Al configurations using measured thickness

Conf.	r_i (in)	Estimated thickness of the 'active' layer (mils)	Measured total thickness (mils)	R (in)	$R - r_i$ (mils)	α	β
6	6.00	9.9	17	6.009	8.5	1.39	1.20
7	4.72	9.6	21	4.740	10.5	0.84	0.90
8	7.28	9.4	24	7.290	12.0	0.67	0.80
9	5.91	9.2	25	5.920	12.5	0.58	0.79

uniformity in these results. The results for the x/Al configurations can be seen in Table 2.

The active to inactive ratio was calculated using the ceramic layer as the active layer, and the metal as the inactive, which predicts configuration 4 as the one that produces the most displacement under no load. To examine this result, the ratio defined as β (see Eq. (3)) was calculated. If β is less than one, the neutral axis is located in the 'inactive' layer and if the ratio is greater than one, the neutral axis is in the 'active' layer. Values for β further show that when the neutral axis is just below the active layer, a large displacement is obtained from the piezoelectric device. This agrees with the theory presented by Furman et al. [25].

The present piezoelectric devices, however, have additional material added between the layers (LaRC-SI™ film). Since the thickness of this adhesive material is difficult to determine, the total thickness of the device was measured using a micrometer. This value was defined as measured thickness. In this manner, an approximate thickness of adhesive layers can be determined. Using this approach, the theory does not predict configuration 4 as the best, but configuration 2. The results obtained are presented in Table 3. For this case, the neutral axis shifts, and the theory no longer agrees with the measurements performed. The inaccuracy in measuring real thickness of the devices, as well as the estimation of the thickness of the adhesive, may explain the discrepancies between the results. Additionally, loading can change neutral axis location in such a manner that some of these configurations perform better under load.

The same calculations were performed for the Al/Al configurations. Using theoretical thicknesses gives the results presented in Table 4, which clearly show the neutral-axis theory to be inaccurate. However, if the measured thicknesses are used, the theory appears to predict the observed results. (See Table 5)

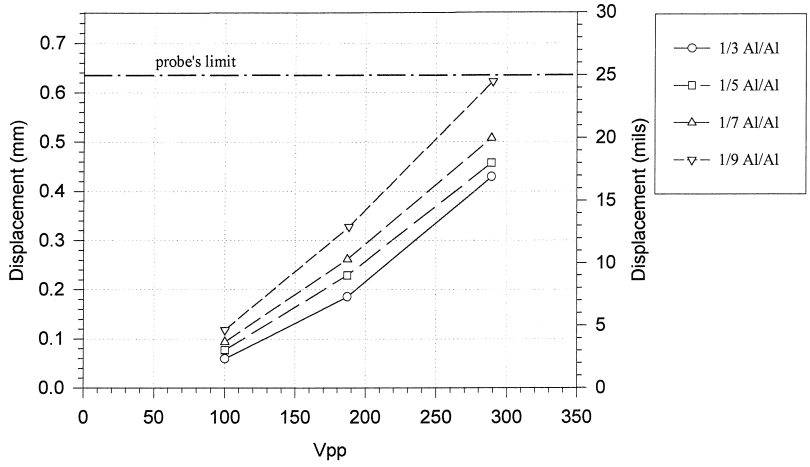

Fig. 8. Displacement vs. voltage at 1 Hz for Al/Al configurations.

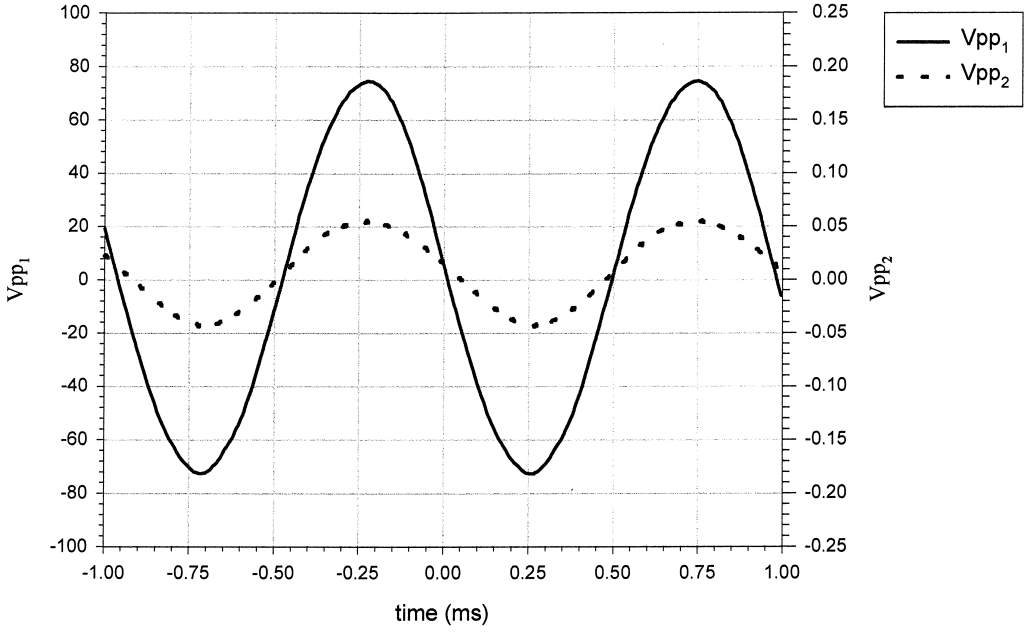

Fig. 9. Driving voltage waveform and displacement waveform for configuration 0/7–x/Al at 1 Hz.

In these configurations, the measured thicknesses of the samples were used to estimate adhesive thickness. These results again show that the configuration producing the most displacement is the one with a $\beta = 1.0$. This theory was applied successfully since the values of the modulus of elasticity of aluminum,

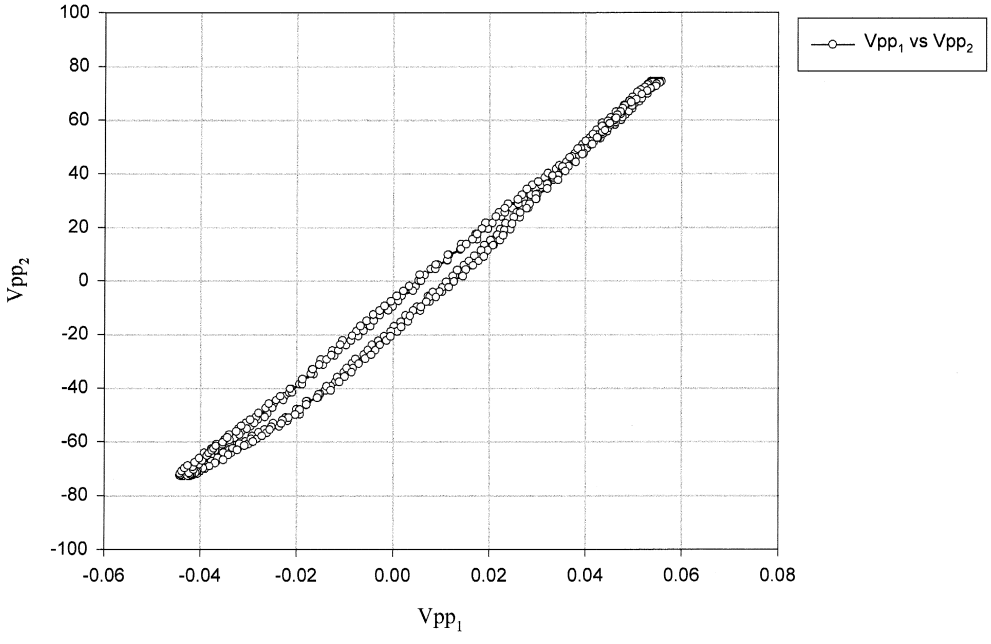

Fig. 10. Hysteresis curve for configuration 0/7–x/Al at 1 Hz.

(aluminum alloy 2024, 73 GPa) [24] and the ceramic wafer (69 GPa) [25] are almost equal, making the stresses equally distributed [23].

Due to the vast amount of data available, displacement as a function of peak-to-peak voltage is only presented at 1 Hz for some of the more relevant configurations. Fig. 8 shows a linear relationship between applied voltage and displacement. Piezoelectric materials have a known hysteresis effect. In order to see if these THUNDER devices reflect this characteristic, the displacement as a function of voltage was plotted. These oscilloscope plots presented as Figs. 9 and 10 show an example of the response of the piezoelectric devices to an applied AC sinusoidal signal. As Fig. 9 shows, at 1 Hz there is no phase shift between the driving voltage (Vpp_1) and the measured displacement (Vpp_2) for configuration 4. Furthermore, the hysteresis is very small at this frequency, as can be seen in Fig. 10.

5. Conclusions

The present results show that in order to obtain accurate displacement measurements for the present devices, they should be poled after processing, even though the ceramic wafer may have been poled at the manufacturer. One of the reasons for depoling might be a result of the Curie point for PZT-5A. This temperature is 350°C, compared to the processing temperature for the piezoelectric devices of 320°C, making the properties of the ceramic (K_{T3}, etc.) less stable.

The experiments have also shown that the present clamping procedure for the piezoelectric devices near the resonant frequency is not appropriate, due to the large displacements obtained at those points. A more compliant clamping device is needed at this value of frequency, which seems to be independent of the configuration tested (approximately 250 Hz).

Further analysis of the data has shown that the movement of the device is restricted when a metal layer is placed on top of the ceramic layer. This phenomenon can be explained by both the location of the neutral axis and the increased tension the additional metallic layer places on the device. A parameter, β, was defined such that $\beta < 1$ indicates that the neutral axis of the static device is in the lower section of the device, or the inactive layer (metal), and when $\beta > 1$, the neutral axis is in the active (ceramic) layer. Then, the configuration that provides the best performance has $\beta = 1$. However, the total thickness of the device should be taken into account (including the adhesive) when calculating β. This theory then appears to fail for the x/Al cases, with measured backing thickness, although it holds for Al/Al configurations.

Acknowledgements

This work was performed under the ODU/NASA Space Act Agreement number SAA-326.

References

[1] D. Dehart, S. Griffin, Astronautical Laboratory Smart Structure/Skins Overview, Proceedings of the First Joint U.S./Japan Conference on Adaptive Structures, Maui, Hawaii, Nov 13–15, 1990, pp. 3–10.
[2] S.K. Ha, C. Kelilers, F. Chang, Finite element analysis of composite structures containing distributed piezoceramic sensors and actuators, AIAA J. 30 (3) (1992) 772–781.
[3] H.S. Tzou, R. Ye, Analysis of piezoelectric structures with laminated piezoelectric triangle shell elements, AIAA J. 34 (1) (1996) 110–115.
[4] C. Suplee, Is the Sky the Limit in the Future? The Virginian-Pilot, Business News, Wednesday, January 8, 1997, p. D-1.
[5] A.J. Zuckerwear, R.A. Pretlow, J.W. Stoughton, D.A. Baker, Development of a piezopolymer pressure sensor for a portable fetal heart rate monitor, IEEE Trans. Biomed. Eng. 40 (9) (1993) 963–969.
[6] S.M. Ehlers, T.A. Weisshaar, Static Aerolastic Behavior of an Adaptive Laminated Piezoelectric Composite Wing, Proceedings of the 31st AIAA/ASME/ASCE/HS/ASC Structures, Structural Dynamics, and Materials Conference, Long Beach, CA, 1990, pp. 1611–1623.
[7] B. Jaffe, W.R. Cook, H. Jaffe, Piezoelectric Ceramics, Academic Press, New York, 1971.
[8] Z. Ounaies, Sol–gel, microwave processing of PZT materials for sensor and actuator applications, Ph.D. Thesis, The Pennsylvania State University, December 1995.
[9] M. Pan, S. Yoshikawa, Design factors in multilayer, Mech. Eng. Mag. (1996) 74–76.
[10] V. Giurgiutiu, Z. Chaudhry, C.A. Rogers, Energy-Based Comparison of Solid-State Actuators, Center for Intelligent Material Systems and Structures, Virginia Polytechnic Institute and State University, Blacksburg VA, Report No. CIMSS 95-101, September 1995.

[11] S. Takahashi, S. Hirose, K. Uchino, Stability of PZT piezoelectric ceramics under vibration level change, J. Am. Ceram. Soc. 77 (9) (1994) 2429–2432.
[12] C.D. Near, Piezoelectric Actuator Technology, Presented at SPIE Smart Structures and Materials Conference, February 27, 1996.
[13] S. Ashley, Smart skis and other adaptive structures, Mech. Eng. Mag. 117 (11) (1995) 76–81.
[14] E. Furman, G. Li, G.H. Haertling, An investigation of the resonance properties of RAINBOW devices, Ferroelectrics 160 (1994) 357–369.
[15] R.G. Bryant, LaRC™-SI: A soluble aromatic polyimide, High Perform. Polym. 8 (1996) 607–615.
[16] E.J. Siochi, P.R. Young, R.G. Bryant, Effect of Molecular Weight on the Properties of A Soluble Polyimide, Proceedings of the 40th International SAMPE Symposium, May 1995, pp. 11–17.
[17] Brute Force Chip, Popular Mechanics, March 1997, p. 16.
[18] THUNDER is Booming, Technology Transfer, NASA News, InTech., August 1996, p. 23.
[19] K. Henry, NASA Rolls Out Award-Winning THUNDER, News Researcher, vol. 10(19), September 20, 1996.
[20] THUNDER Actuators Move a Lot, R&D Magazine, vol. 38(10), September 1996, p. 44.
[21] NASA Langley Develops Piezoelectric Material, Aviation Week and Space Technology, vol. 145(15), October 1996, p. 10.
[22] E. Furman, G. Li, G.H. Haertling, Electromechanical Properties of RAINBOW Devices, Proceedings of the 9th IEEE International Symposium on Applications of Ferroelectrics, August 1994, pp. 146–149.
[23] R.C. Hibbeler, Mechanics of Materials, 3rd ed., Prentice Hall, NJ, 1997.
[24] W.D. Pilkey, Formulas for Stress, Strain, and Structural Matrices, John Wiley and Sons, 1994, p. 174.
[25] PZT Piezoelectric Materials, Technical Data, MOTOROLA, 1996.